

Testing left-right symmetry with inverse seesaw at the LHC

Mathew Thomas Arun,^{1,*} Tanumoy Mandal,^{1,†} Subhadip Mitra,^{2,‡}
Ananya Mukherjee,^{3,§} Lakshmi Priya,^{1,4} and Adithya Sampath¹

¹Indian Institute of Science Education and Research Thiruvananthapuram, Vithura, Kerala, 695 551, India

²Center for Computational Natural Sciences and Bioinformatics,

International Institute of Information Technology, Hyderabad 500 032, India

³Department of Physics, University of Calcutta, 92 Acharya Prafulla Chandra Road, Kolkata 700 009, India

⁴Deutsches Elektronen-Synchrotron DESY, Notkestr. 85, 22607 Hamburg, Germany

(Dated: September 21, 2021)

In the left-right symmetric models, a heavy charged gauge boson W' can decay to a lepton and a right-handed neutrino (RHN). If the neutrino masses are generated through the standard type-I seesaw mechanism, the Yukawa couplings controlling two-body decays of the RHN become very small. As a result, the RHN decays to another lepton and a pair of jets via an off-shell W' . This is the basis of the Keung-Senjanović (KS) process, which was originally proposed as a probe of lepton number violation at the LHC. However, if a different mechanism like the inverse seesaw generates the neutrino masses, a TeV-scale RHN can have large Yukawa couplings and hence, dominantly decay to a lepton and a W boson, leading to a kinematically different process from the KS one. We investigate the prospect of this unexplored process as a probe of the inverse seesaw mechanism in the left-right symmetric models at the HL-LHC. Our signal arises from the Drell-Yan production of a W' and leads to two high- p_T same-flavour-opposite-sign leptons and a boosted W -like fatjet in the final state. We find that a sequential W' with mass up to ~ 6 TeV along with a TeV-scale RHN can be discovered at the HL-LHC.

I. INTRODUCTION

The neutrino oscillation data unambiguously establish that neutrinos have tiny but nonzero masses, the explanation of which calls for physics beyond the Standard Model (SM). Among the various extensions of the SM, the left-right symmetric models (LRSMs) provide a natural framework to embed the right-handed neutrinos (RHNs) and generate the neutrino masses. In this framework, parity violation is a low-energy feature; parity invariance is restored at high energies. Hence, the SM gauge group is extended to $SU(3)_C \otimes SU(2)_L \otimes SU(2)_R \otimes U(1)_{B-L}$ in the LRSM and the left-right symmetry breaks at the TeV-scale introducing two heavy gauge bosons, W' and Z' in the spectrum.

A simple method to generate the small masses of the left-handed neutrinos is the seesaw mechanism, where one introduces a set of heavy SM-singlet Majorana fermions breaking the $(B-L)$ -symmetry. However, the mechanism relies on a very high-scale explicit breaking of the lepton number symmetry in its simplest form (type-I seesaw). Hence, in this case, one requires the new physics scale M to be of the order of 10^{14} GeV, i.e. much beyond the reach of colliders, to arrive at the observed neutrino mass scale $\nu^2/M \lesssim 0.1$ eV without fine-tuning the Higgs vacuum expectation value (VEV, v). From a collider perspective, a much interesting possibility appears when one considers the inverse seesaw mechanism (ISM) [1, 2]. In the ISM, one obtains the

sub-eV neutrinos by adding three extra singlet Majorana fermions with mass $\mu \sim \text{keV}$ [3, 4] with the three TeV-range RHNs.

In this paper, we investigate an interesting collider signature of a minimal realisation of LRSM with ISM. We consider the $pp \rightarrow W'$ process where W' is a heavy charged gauge boson which decays to a charged lepton (ℓ) and a RHN (N_R). The heavy RHN then further decays to a W boson and another charged lepton. For this decay to occur, we need $M_{N_R} < M_{W'}$, a mass ordering possible to obtain with the ISM. When the W , produced in the decay of N_R , decays hadronically, the process becomes similar to the Keung-Senjanović (KS) process [5], which was proposed as a direct probe of the Majorana nature of the RHNs in the LRSM. The KS process also acts as a clean probe of the heavy right-handed W' and, thus, the TeV-range breaking of the left-right symmetry. In the original KS process, the mass of RHN was taken to be lighter than the mass of W' , i.e. $M_{W'} > M_{N_R}$. In this process, a RHN, produced along with a charged lepton through the Drell-Yan production of W' , decays to a charged lepton and two jets through an off-shell W' , as shown in Fig. 1(a). If, however, $M_{W'} < M_{N_R}$, a similar final state would arise, but in this case, N_R would be produced through an off-shell W' and decay through an on-shell W , as shown in Fig. 1(b). Either way, we would get the same $\ell\ell jj$ final state in both cases [6–23].

Our signature differs from the KS process mainly in the fact that in our case, the RHN decays to an on-shell W [in particular, $N_R \rightarrow \ell W_h$, where W_h denotes a hadronically decaying W , see Fig. 1(c)] as opposed to a W' (off-shell or on-shell). In regular LRSM with type-I seesaw, the Yukawa couplings responsible for the two-body decays, $N_R \rightarrow \ell W$ are extremely small for TeV-scale RHNs.

* mathewthomas@iisertvm.ac.in

† tanumoy@iisertvm.ac.in

‡ subhadip.mitra@iiit.ac.in

§ ananyatezpur@gmail.com

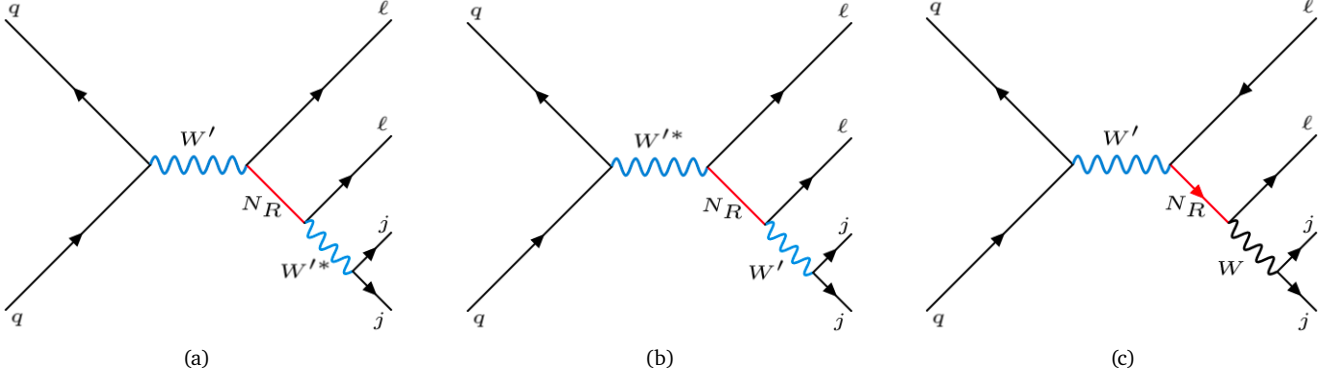


FIG. 1. Feynman diagrams for the KS Process: (a) for $M_{W'} > M_{N_R}$ and (b) for $M_{W'} < M_{N_R}$. Our signal process with $M_{W'} > M_{N_R}$ and the decay of N_R through on-shell W is shown in (c).

Particle	$SU(3)_C$	$SU(2)_L$	$SU(2)_R$	$U(1)_{B-L}$
$q_L^i \equiv \begin{pmatrix} u_L^i \\ d_L^i \end{pmatrix}$	3	2	1	$\frac{1}{3}$
$q_R^i \equiv \begin{pmatrix} u_R^i \\ d_R^i \end{pmatrix}$	3	1	2	$\frac{1}{3}$
$L_L \equiv \begin{pmatrix} \nu_L^i \\ e_L^i \end{pmatrix}$	1	2	1	-1
$L_R \equiv \begin{pmatrix} N_R^i \\ e_R^i \end{pmatrix}$	1	1	2	-1
S^i	1	1	1	0
$\Phi = \begin{pmatrix} \phi_1^0 & \phi_2^+ \\ \phi_1^- & \phi_2^0 \end{pmatrix}$	1	2	2	0
$\chi_L = \begin{pmatrix} \chi_L^+ \\ \chi_L^0 \end{pmatrix}$	1	2	1	1
$\chi_R = \begin{pmatrix} \chi_R^+ \\ \chi_R^0 \end{pmatrix}$	1	1	2	1

TABLE I. Particle content of left-right symmetric model based on the gauge group $SU(3)_C \otimes SU(2)_L \otimes SU(2)_R \otimes U(1)_{B-L}$.

As a result, such decays become negligible compared to off-shell W' mediated three-body decay. However, with the ISM, the Yukawa couplings that govern the $N_R \rightarrow \ell W$ decay can be sufficiently large such that the signature is observable at the LHC. Even though the final state of this process is essentially the same as that of the KS one, the kinematics of these two processes are very different. In our signal, the jet-pairs come from the decay of boosted W and form a fatjet. This feature is not present in the KS process. Hence, the two processes complement each other and can be used to probe different neutrino mass generation mechanisms. Unlike the KS process, the $N_R \rightarrow \ell W_h$ signature has not been searched for at the LHC.

The paper is organised as follows. In Section II, we discuss the model and neutrino parameters, in Section III, we compare our signature and the KS process in more detail, in Section IV, we discuss the LHC bounds on W' , in Section V, we analyse our signature, and finally, in Section VI, we conclude.

II. LEFT-RIGHT SYMMETRY WITH INVERSE SEESAW

We consider a simple realisation of the LRSM with the following gauge structure,

$$\mathcal{G}_{LRSM} = SU(3)_C \otimes SU(2)_L \otimes SU(2)_R \otimes U(1)_{B-L}. \quad (1)$$

In this model, the $SU(2)_R$ gauge coupling g_R is a free parameter; not same as the $SU(2)_L$ gauge coupling g_L . The particle content and the gauge quantum numbers are summarised in Table I. In addition to the SM fermions, there are three right-handed neutrinos (N_R^i) and three neutral fermions (S^i) introduced for the three generations. The RHNs are naturally present in the LRSM, whereas the neutral fermions are required to realise the ISM. The RHNs form the $SU(2)_R$ doublets with the right-handed charged leptons, whereas the S^i are all singlets under \mathcal{G}_{LRSM} . The enlarged scalar sector consists of three multiplets, i.e., the Higgs bidoublet Φ and two doublet scalars χ_L and χ_R which are doublets under $SU(2)_L$ and $SU(2)_R$ gauge groups, respectively.

A. Symmetry breaking

The spontaneous breaking of the gauge symmetry follows the pattern below

$$\begin{aligned} &SU(3)_C \otimes SU(2)_L \otimes SU(2)_R \otimes U(1)_{B-L} \\ &\quad \downarrow \langle \chi_R \rangle \\ &SU(3)_C \otimes SU(2)_L \otimes U(1)_Y \\ &\quad \downarrow \sqrt{\langle \Phi \rangle^2 + \langle \chi_L \rangle^2} \\ &SU(3)_C \otimes U(1)_{EM}. \end{aligned}$$

The doublet field χ_R is non-trivially charged under $SU(2)_R \times U(1)_{B-L}$. Hence, when it acquires a TeV-scale VEV, the group breaks down to $U(1)_Y$ and gives masses to the charged W' and neutral Z' bosons. The standard electroweak symmetry breaking is then carried out by

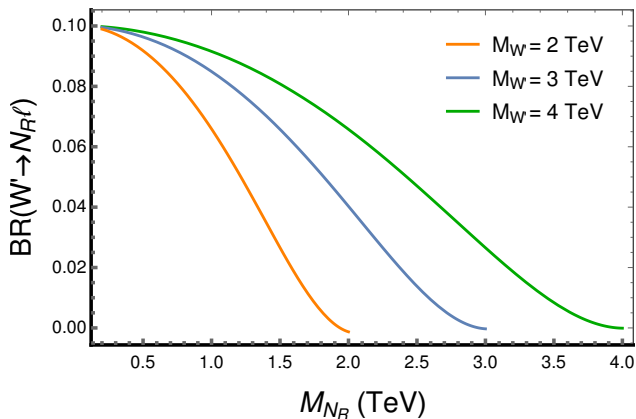


FIG. 2. Branching ratio of $W' \rightarrow N_R \ell$ as functions of M_{N_R} for different $M_{W'}$ choices.

the neutral scalar fields in χ_L and the bidoublet Φ satisfying the relation,

$$\sqrt{\langle \chi_L^0 \rangle^2 + \langle \phi_1^0 \rangle^2 + \langle \phi_2^0 \rangle^2} \sim 246 \text{ GeV}. \quad (2)$$

The electromagnetic charge can be expressed as

$$Q_{EM} = I_{3L} + I_{3R} + \frac{B-L}{2}. \quad (3)$$

Since here our motivation is to study the unexplored signature as discussed in the introduction, we make an assumption that the W' boson dominantly decays to the SM fermions and RHNs. We make a further simplifying assumption that two of the RHNs are heavier than W' , so that the vector boson can decay to only one generation of RHNs. Since, W' universally couples to right-handed fermions with the strength g_R , the branching ratio (BR) of the $W' \rightarrow N_R \ell$ decay is about 10% in the $M_{W'} \gg M_{N_R}$ limit, as seen in Fig. 2. As the mass of the RHN goes close to $M_{W'}$, the BR of the $N_R \ell$ mode falls due to phase space reduction.

B. Inverse seesaw mechanism

In the original ISM, three TeV-scale RHNs and three extra singlet neutral fermions S_L^i (where $i \in \{1, 2, 3\}$) are added to the three active neutrinos ν_L^i . The tiny neutrino masses are generated from the mixing between the N_R^i and S_L^i states:

$$\mathcal{L} = Y \bar{L}_L \tilde{H} N_R + M_R \overline{(N_R)^c} S_L^c + \frac{1}{2} \mu \bar{S}_L (S_L)^c + \text{h.c.}, \quad (4)$$

where $\tilde{H} = i\sigma_2 H^*$, the superscript ' c ' denotes charge conjugation, and we have suppressed the generation index.

In the left-right symmetric realisation of the ISM, the lepton masses are generated via a Yukawa Lagrangian,

$$\begin{aligned} \mathcal{L}_Y = & -Y \bar{L}_R \Phi^\dagger L_L - \tilde{Y} \bar{L}_R \tilde{\Phi}^\dagger L_L - Y_1 \bar{S} \tilde{\chi}_L^\dagger L_L - Y_1 \bar{S}^c \tilde{\chi}_R^\dagger L_R \\ & - \frac{1}{2} \mu \bar{S}^c S + \text{h.c.}, \end{aligned} \quad (5)$$

where Y, \tilde{Y}, Y_1 are the 3×3 Yukawa couplings and μ is the 3×3 Majorana mass matrix. In the above Lagrangian, $\tilde{\chi}$ and $\tilde{\Phi}$ represent the charge conjugated fields. The complete mass matrix in the basis (ν_L, N_R^c, S^c) obtained from Eq. (5) reads as

$$M_\nu = \begin{pmatrix} 0 & m_D^T & m_D'^T \\ m_D^T & 0 & M_R^T \\ m_D' & M_R & \mu \end{pmatrix}, \quad (6)$$

where

$$\begin{aligned} m_D &= \frac{1}{\sqrt{2}} \left(Y \langle \phi_1^0 \rangle + \tilde{Y} \langle \phi_2^0 \rangle \right), & m_D' &= \frac{1}{\sqrt{2}} Y_L \langle \chi_L^0 \rangle, \\ M_R &= \frac{1}{\sqrt{2}} Y_R \langle \chi_R^0 \rangle. \end{aligned}$$

The light-neutrino mass can be found by a block diagonalisation of the mass matrix in the limit $\langle \phi_1^0 \rangle \gg \langle \phi_2^0 \rangle$ as,

$$m_\nu \sim \frac{\langle \chi_L^0 \rangle}{\langle \chi_R^0 \rangle} \left(m_D + m_D^T \right) - m_D (M_R^T)^{-1} \mu M_R^{-1} m_D^T. \quad (7)$$

The first term is the linear seesaw contribution and a consequence of the left-right symmetry. The experimentally observed neutrino mass squared differences and mixing angles predict this term to be subdominant, $\langle \chi_L^0 \rangle / \langle \chi_R^0 \rangle \lesssim 10^{-12}$. Even if χ_L^0 is generated radiatively at one loop, it remains small and satisfies the above condition for $\mu \sim \mathcal{O}(1)$ keV and $\langle \chi_R \rangle \sim 10^4$ GeV [24].

The novelty of the ISM with a TeV scale RHN lies in the double suppression by the mass scale associated with the mass scale M . To have a sub-eV neutrino mass scale with m_D at the electroweak scale, one should have M at the TeV scale and μ at the keV scale. The tiny μ ensures the neutrino mass to be small. As $\mu \rightarrow 0$, the lepton number symmetry is restored leading to $m_\nu \rightarrow 0$. The neutrino Yukawa couplings can be obtained using the extended Casas-Ibarra formalism derived in [25], based on the original formalism [26],

$$Y_\nu = \frac{1}{v} U m_\nu^{1/2} R \mu^{-1/2} M_R^T, \quad (8)$$

with the matrices $m_\nu = \text{diag}(m_1, m_2, m_3)$ and $M_R = \text{diag}(M_{R_1}, M_{R_2}, M_{R_3})$, carrying the light-neutrino mass eigenvalues and the heavy Majorana neutrino masses, respectively. Here, R is a complex orthogonal matrix in general and U is the Pontecorvo-Maki-Nakagawa-Sakata matrix characterising the mixing among leptons¹.

We numerically evaluate the Yukawa couplings using Eq. (8). We use the best-fit central values of all the oscillation parameters tabulated in [30]. A flavour symmetric realisation of such a model based on the left-right

¹ For some recent implications of this kind of formalism, readers may see Refs. [27–29].

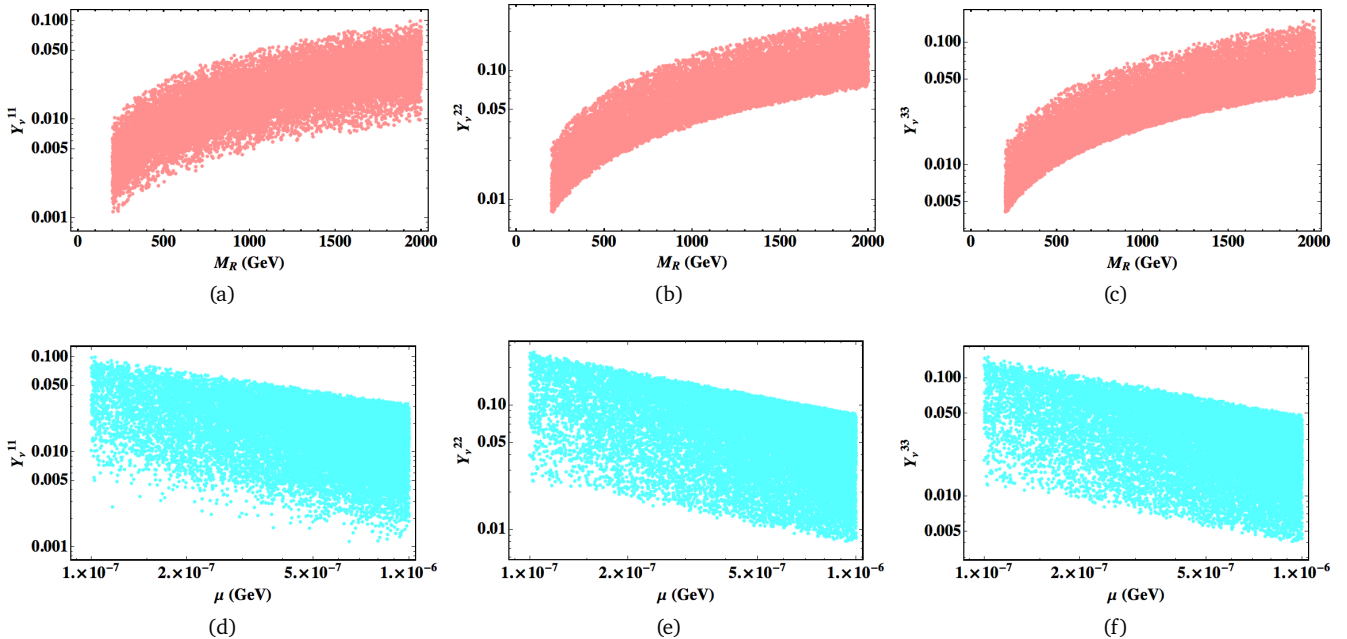


FIG. 3. The Yukawa couplings versus RHN mass (top row) and the lepton number violating scale μ (bottom row) in the inverse seesaw scheme

symmetry would restrict the neutrino oscillation parameters [31, 32]. We follow [26] for the parametrisation of the rotational matrix (R). In general, R can take any complex value for the mixing angles. However, we assume that the three angles in the rotational matrix are real for simplicity and choose them as $x = \pi/3$, $y = \pi/4$, and $z = \pi/5$ for a benchmark set of values. There is, however, nothing special about this particular set of values as our phenomenological analysis is mostly insensitive to the choice of these parameters.

In Fig. 3, we show the dependence of the Yukawa couplings on the heavy RHN mass scale M_R (top row) and the lepton number violating scale μ (bottom row). We see that the Yukawa couplings increase with M_R and decrease with μ from this figure [and also Eq. (8)]. The order of magnitude of μ has a very crucial role in determining the degree of degeneracy among the RHN mass eigenstates obtained in the ISM. The keV-scale μ also plays an important role in resonant leptogenesis [33].

The BRs of the two-body decay modes of the RHNs, namely, $W^\pm \ell$, $Z\nu$ and $H\nu$, are determined by the Yukawa couplings shown in Fig. 3. There is also a three-body decay mode of N_R through an off-shell W' present in LRSM. As explained before, the three-body decay is the dominant mode in the standard type-I seesaw where the Yukawa couplings controlling the two-body decays are very small. In this case, the KS process becomes important. With the ISM, the Yukawa couplings become large and hence, the two-body decays of N_R through on-shell W' take over the three-body decays. Usually, the BRs of N_R to $W\ell$, $Z\nu$ and $H\nu$ are in the proportion 2 : 1 : 1 when the mass of N_R is sufficiently above the kinematic threshold of these decays. In our analysis, we have taken

the BRs of N_R in that proportion. The pair production of RHNs through an s -channel Z' is also possible in our model (some discussion on the prospects of that channel can be found in [34–37] in the context of $U(1)$ extended models). This will be discussed in an upcoming paper in a general context. Our signal is actually insensitive to the actual values of the Yukawa couplings. This can be probed with high-precision in an electron-positron collider [38].

III. SIGNAL TOPOLOGY AND THE KS PROCESS

The KS process gives rise to the $\ell\ell jj$ final state. This process is well known and has been searched for by both the ATLAS and CMS collaborations (see, e.g., [39, 40]). When $M_{W'} < M_{N_R}$, the process is kinematically suppressed and hence, difficult to probe. The $M_{W'} \gtrsim M_{N_R}$ region is accessible and can be further categorised into two kinematic regions – resolved and merged [23]:

- (a) When the RHN is not much lighter than W' , i.e., $0.1M_{W'} \lesssim M_{N_R} < M_{W'}$, the two jets from the W'^* decay can be resolved. This leads to two isolated leptons and at least two high p_T jets. This process is fully reconstructible: the jj system along with one lepton can be used to reconstruct the N_R . The invariant mass of the $\ell\ell jj$ system forms a peak around W' mass.
- (b) In the merged topology, $M_{N_R} \lesssim 0.1M_{W'}$. Here, the RHN will be produced with a large boost in the transverse plane. Therefore, the decay of the RHN (i.e. $N_R \rightarrow \ell W'^* \rightarrow \ell jj$) will be highly collimated

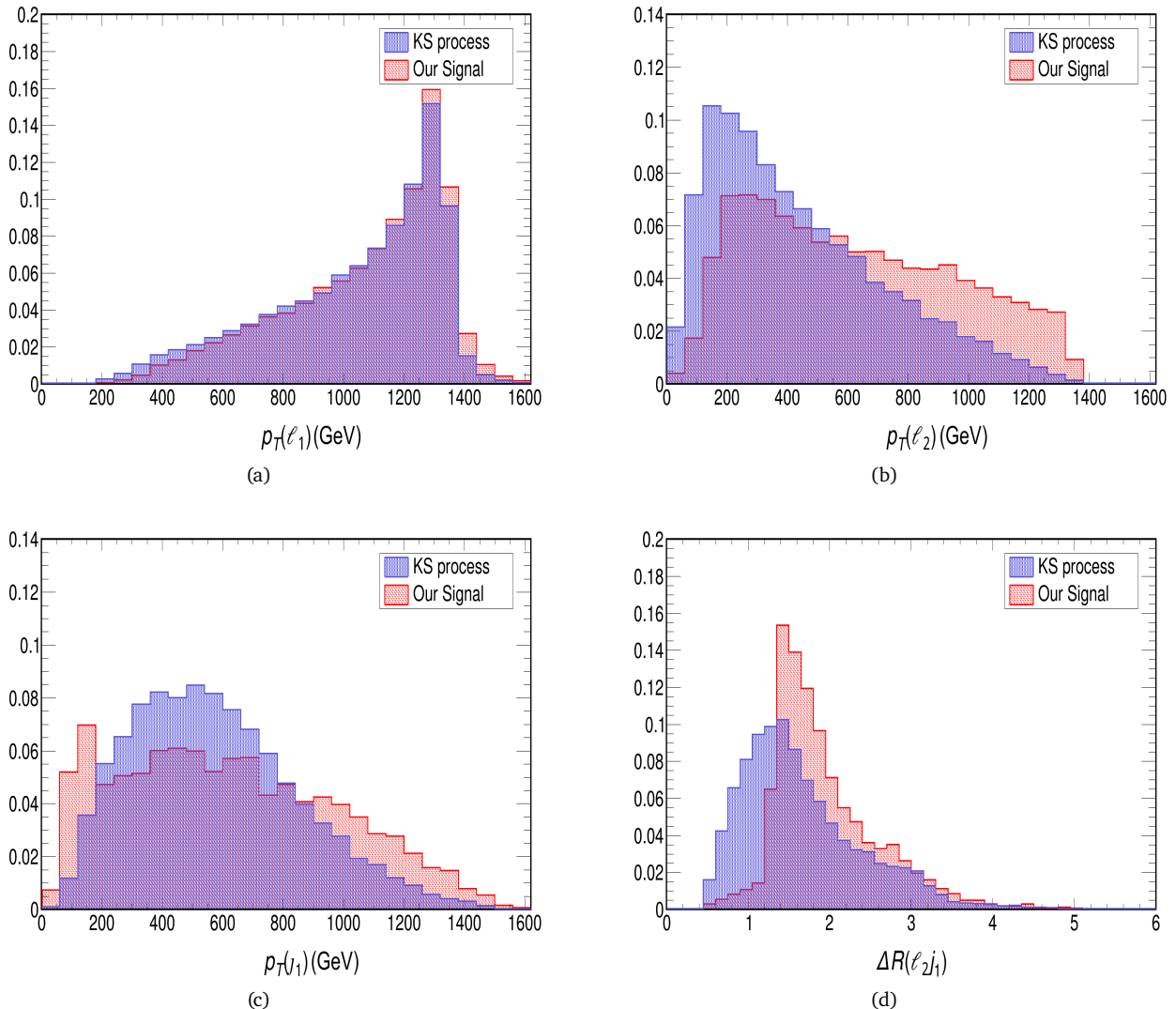


FIG. 4. Comparison of various kinematic distributions of the KS process and our signal. These distributions are obtained for $M_{W'} = 3$ TeV and $M_{N_R} = 1$ TeV benchmark masses with $g_R = 0.1$.

and produce a fatjet that can be used for reconstructing the N_R wholly or at least, partially. This will give rise to one lepton and a N_R -jet (J_{N_R}). If the RHN is long-lived, it will lead to a displaced vertex signature, i.e. its decay length roughly would lie in the range $[10^{-3} - 1]$ m. In this case the merged J_{N_R} appears at a distance visibly away from the primary vertex. If N_R decays outside the detector, it produces the invisible signature.

For our study, we also consider the $M_{W'} > M_{N_R}$ kinematic region but, in our case, the RHN decays through an on-shell W boson [Fig. 1(c)]. More specifically, a W' boson, produced from the pp collision, decays into a μ^- or a μ^+ and the second generation RHN, N_R^2 (we choose the second generation because muons have better identification efficiency at the LHC than electrons and taus.) Since we assume the other RHNs, i.e., N_R^1 and N_R^3 , are heavier than W' , it cannot decay to these RHNs. The Majorana nature of N_R^2 allows it to decay

into a μ^- and a W^+ or a μ^+ and a W^- with equal probability. The W boson then decay hadronically to two jets. Thus the final state particles include two leptons (either same-sign, signalling a violation of lepton number, or different-sign) and two jets (or a W_h). That the kinematics of this process is different from that of the KS process can be seen in the distributions shown in Fig. 4. Therefore, it demands a different treatment.

IV. EXISTING W' SEARCHES AND BOUNDS

We briefly review here the recent LHC direct search limits on W' . In experimental searches, decays of W' to different fermionic modes ($\ell\nu$, jj , $t\bar{b}$ and $N\ell$) and diboson modes (WZ and WH) are considered, in our model, the $W \leftrightarrow W'$ mixing suppresses the $W' \rightarrow \ell\nu, WZ, WH$ mode whereas the other decay modes, controlled by g_R , are not mixing angle suppressed.

Searches for the KS process: Recently, the CMS collab-

Experiment	Luminosity (fb ⁻¹)	Observed limit (TeV)
ATLAS dijet [46]	139	3.80
CMS dijet [47]	137	3.60
ATLAS $t\bar{b}$ [49]	36.1	3.45
CMS $t\bar{b}$ [50]	137	3.50

TABLE II. Summary of the 95% CL exclusion limits on W' obtained from recasting the LHC experiments (assuming only one RHN decay mode of W' is open).

oration has performed a search for the KS process in the final states containing a pair of same-flavour charged leptons (e or μ , with the same or opposite electric charges) and two jets [40] at $\sqrt{s} = 13$ TeV with 137 fb⁻¹ integrated luminosity. Assuming $g_L = g_R$, the search excludes W' with mass up to ~ 5 TeV with 95% confidence level (CL). Earlier, the ATLAS collaboration has searched for the resolved [39] and merged [41] topologies and obtained similar exclusion limits. Ref [42] puts a lower limit of 3.5 TeV on the mass of W' (assuming the mass of the third-generation RHN to be the half of $M_{W'}$) from the search for the KS process in the $\tau\tau jj$ final state. (A slightly different process where the W'' 's in the KS process are replaced by W 's is considered in [43]. This process is sensitive to the Yukawa couplings involved in the $N_R \rightarrow \ell W$ decay. The same process can also lead to displaced vertex signature if the decay width of N_R is small [44, 45].)

Searches for a dijet resonance: Both ATLAS and CMS have searched for a jj resonance [46, 47] at the 13 TeV LHC with 139 and 137 fb⁻¹ of integrated luminosities, respectively. The ATLAS search rules out a sequential W' with $M_{W'} \lesssim 4$ TeV and the CMS study rules out $M_{W'} \lesssim 3.6$ TeV. We have recast the observed limits from these two searches to obtain bounds on g_R , as shown in Figs. 5(a) and 5(b). In the ATLAS search recast, we have appropriately factored in the variation of detector acceptance (A) with $M_{W'}$. However, we have assumed a flat $A = 0.5$ for the CMS search recast.

Searches for a $t\bar{b}$ resonance: The ATLAS collaboration has presented a combined exclusion limit for the W' decaying through the $t\bar{b}$ final state, with hadronic [48] and leptonic [49] top decays with 36.1 fb⁻¹ integrated luminosity at the 13 TeV LHC. For a sequential W' model, $M_{W'} \lesssim 3.15$ TeV has been ruled out at 95% CL. The CMS collaboration also has performed the search for a W' decaying into a $t\bar{b}$ pair, in the all-hadronic mode using the 13 TeV LHC data with 137 fb⁻¹ of integrated luminosity [50]. The CMS search excludes the W' masses below 3.4 TeV. We recast these limits as well [see Figs. 5(a) and 5(b)].

We summarise the dijet and $t\bar{b}$ resonance limits obtained after recasting the searches, under the assumption that only one RHN decay mode is open, in Table IV.

Other searches: There are other searches for W' in var-

ious decay channels. For example, the charged lepton + missing transverse energy channel [51–54] the WH channel [55–58], the WZ channel [57–60], etc. However, all these decays occur through W - W' mixing which is small in the LRSM. Hence, these searches do not constrain the parameter space of our model.

In principle, as demonstrated in Refs. [61–64], one can also recast other searches in the $\ell\ell jj$ channel (e.g., the leptoquark searches) to obtain bounds. Here, however, we ignore such bounds on W' , as such limits are expected to be weaker than the direct ones.

V. RHN DECAYS THROUGH A W BOSON

We implement the Lagrangian terms relevant for the productions and decays of W' and N_R in FEYN-RULES [65], and obtain the UFO [66] model files. We use the NNPDF2.3 parton distribution functions (PDFs) to generate signal and the SM background events in MADGRAPH5 [67]. The generated events are passed through PYTHIA8 [68] for showering and hadronisation to DELPHES [69] for detector simulation. We use the anti- k_t jet clustering algorithm [70] in FASTJET [71] to cluster jets from the tower objects. We use two types of jets in our analysis, namely, AK4-jets with jet radius parameter $R = 0.4$ and AK8-fatjets with $R = 0.8$ [72]. In this paper, we use the symbol ' j ' for AK4-jets and ' J ' for AK8-fatjets. We tag b -jets from the AK4-jets.

The process of our interest is given as

$$pp \rightarrow (W')^\pm \rightarrow N_R \ell^\pm \rightarrow (W_h^\pm \ell^\mp) \ell^\pm \quad (9)$$

where, as mentioned before, W_h^\pm denotes a hadronically decaying W -boson. Depending on the masses of the W' and N_R , the W_h can be sufficiently boosted and form a two-pronged fatjet. We employ jet-substructure techniques to tag a boosted W_h with high efficiency. Due to the pseudo-Dirac nature of the N_R , we only have opposite-sign dilepton accompanied by a boosted W -jet in the final state in our case. Leptons originating in the decays of a TeV-scale W' or N_R will also have high transverse momenta (p_T). Therefore, the signature our signal would be two high- p_T same flavor opposite-sign leptons and a W -like two-pronged fatjet. Since there is no missing energy, our signal channel is fully-reconstructible, in principle.

A. The background processes

The following SM processes with large cross sections form the relevant background of our signal.

- $Z + jets$: This process forms the dominant background. We generate it by simulating the $pp \rightarrow Z/\gamma \rightarrow \ell\ell$ process matched up to two extra partons. Here, the two high- p_T leptons can arise from the leptonic decays of the Z -boson, and the QCD jets

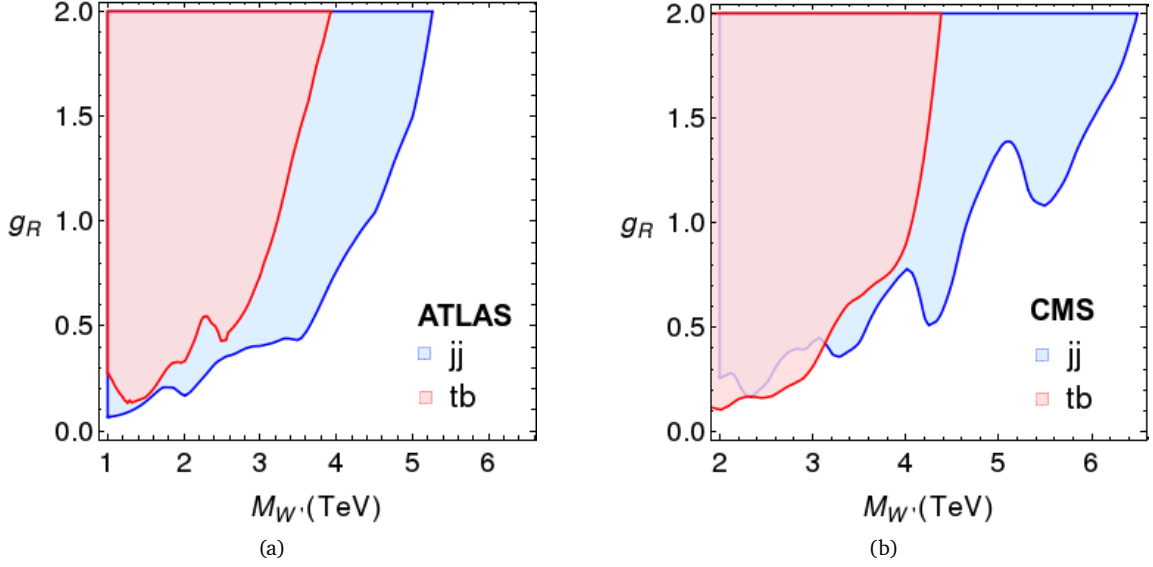


FIG. 5. Exclusion regions in the $M_{W'}-g_R$ plane obtained by recasting the dijet and tb resonance search results by ATLAS and CMS.

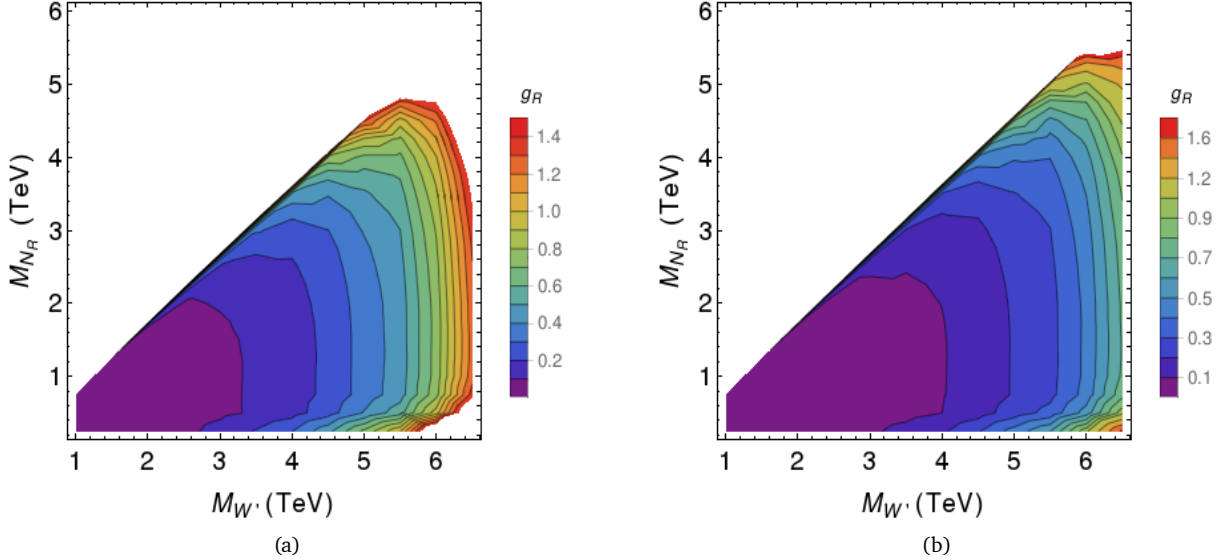


FIG. 6. The regions in the $M_{W'}-M_{N_R}$ plane that can be (a) discovered with 5σ significance and (b) excluded with 2σ significance at the HL-LHC. The contours are for different g_R values. In the left (right) plot, the regions with same colour can be discovered (excluded) with 5σ (2σ) significance or more.

can be misidentified as the W -like fatjet. Since the invariant mass of the two leptons peaks at the Z mass, this background is controlled by a Z -mass veto.

- $tt + jets$: The SM top pair production can also provide us two high- p_T leptons when both the tops decay leptonically. Additionally, a W -like jet can come from the QCD jets. The contribution of this process in the background is significant in our case. We generate the $t\bar{t}$ events by matching the parton showers (PS) with up to two additional jets.
- $tW + jets$: The SM $pp \rightarrow tW$ process contains two

leptons in the final state when both the top quark and the W boson decay leptonically. This process also contributes significantly to the backgrounds of our signal. In this case as well, the W -like jet arises from the QCD jets. We generate this process by jet-PS matching up to two extra jets.

- $VV + jets$: Here, V denotes a W or a Z boson. There are four types of diboson processes, viz., $W_\ell W_\ell$, $W_h Z_\ell$, $Z_\ell Z_h$ and $Z_\ell H_h$ (the subscripts ' ℓ ' and ' h ' represent leptonic and hadronic decay modes) that can act as sources of two high- p_T leptons. In these cases, the W -like jet arises from the hadronic decay of a V or QCD jets. Processes containing

Background processes		σ (pb)	QCD order
V + jets [73, 74]	Z + jets	6.33×10^4	NNLO
tt [75]	tt + jets	988.57	N ³ LO
Single t [76]	tW	83.10	N ² LO
VV + jets [77]	WW + jets	124.31	NLO
	WZ + jets	51.82	NLO
	ZZ + jets	17.72	NLO
ttV [78]	ttZ	1.05	NLO+NNLL
	ttW	0.65	NLO+NNLL

TABLE III. Total cross sections without any cut for the SM background processes considered in our analysis. The higher-order QCD cross sections are taken from the literature and the corresponding orders are shown in the last column. We use these cross sections to compute the K factors which we multiply with the LO cross sections to include higher-order effects.

leptonically decaying Z can be tamed by applying the Z -mass veto on the invariant mass of the lepton pair. Among all the diboson processes, the $W_\ell W_\ell$ process contribute maximally. We generate matched event samples (including up to two extra jets) of these processes. The total diboson contribution, however, is negligible after all the cuts.

- ttV : The SM processes producing a top pair and a vector boson can act as backgrounds for our signal. We consider the following four cases, viz., $t_\ell t_\ell Z_h$, $t_h t_h Z_\ell$, $t_\ell t_\ell W_h$ and $t_\ell t_h W_\ell$ depending on the decays of the tops and vector boson. We generate these event samples without adding extra jets in the final state. Just like the diboson background, this background too contributes negligibly to the total background after the cuts.

We generate all the background processes discussed above at the leading order with MadGraph5. The relevant background processes and their cross sections (at the highest order in QCD available in the literature) are listed in Table III. From the cross sections, we compute the K -factors to incorporate the higher-order effects in our analysis. Before cuts, some of the background processes are large. But, since our signal belongs to a specific region of the phase space, we generate all the background processes with some strong generation level cuts to save computation time. Technically this might lead to a small bias in the event samples. We, however, ignore it for simplicity. The generation level cuts which we use are:

- Transverse momentum (p_T) on the leptons: $p_T(\ell_1), p_T(\ell_2) > 100$ GeV.
- Invariant mass of the lepton pair $M(\ell_1, \ell_2) > 120$ GeV.

The leptons are ordered according to their p_T . The cut on $M(\ell_1, \ell_2)$ is applied to reduce the background involving $Z \rightarrow \ell\ell$ decay (the Z -mass veto).

B. Signal selection

For the final selection, we have divided the signal into low mass ($M_{W'} < 3$ TeV) and high mass ($M_{W'} > 3$ TeV) regions. As explained before, we demand two opposite-sign same flavour leptons and at least one W -like AK8-fatjet. The following selection cuts have been used for the two regions.

Low mass region ($M_{W'} < 3$ TeV):

1. Transverse momentum on leptons, $p_T(\ell_1) > 300$ GeV, $p_T(\ell_2) > 100$ GeV.
2. Invariant mass of the lepton pair, $M(\ell_1, \ell_2) > 200$ GeV.
3. Scalar sum of p_T of all visible objects, $S_T > 0.6 \times M_{W'}$.
4. Missing transverse energy, $\cancel{E}_T < 100$ GeV.
5. Mass of the leading AK8-fatjet, $|M(J_1) - M_W| < 20$ GeV.
6. N -subjettiness ratio of the leading AK8-fatjet, $\tau_{21}(J_1) < 0.35$.
7. Invariant mass on the leading AK8-fatjet and dilepton system, $|M(J_1, \ell_1, \ell_2) - M_{W'}| < 200$ GeV.

High mass Region ($M_{W'} > 3$ TeV):

1. Cut-1 and cut-2 of the low mass region.
2. Scalar sum of the transverse p_T of all visible objects, $S_T > 1500$ GeV
3. Invariant mass on the leading fatjet and dilepton system $M(J_1, \ell_1, \ell_2) > 0.8 \times M_{W'}$ (for $M_{W'} < 5.5$ TeV) and $M(J_1, \ell_1, \ell_2) > 4400$ GeV (for $M_{W'} \geq 5.5$ TeV)

C. Signal significance

After applying the above cuts, let the number of surviving signal and background events at a given luminosity be denoted by N_S and N_B , respectively. From these, one can get an estimation of the statistical significance of the signal from the formula below:

$$\mathcal{Z} = \sqrt{2(N_S + N_B) \ln \left(\frac{N_S + N_B}{N_B} \right)} - 2N_S. \quad (10)$$

We estimate \mathcal{Z} for the HL-LHC, i.e., for 3 ab^{-1} integrated luminosity and $\sqrt{s} = 14$ TeV. Fig. 6 shows the projected discovery (5σ significance) and 2σ exclusion regions in the $M_{W'}$ - M_{N_R} plane. Our signal process mainly depends on three model parameters. Among them, $M_{W'}$ and M_{N_R} are kinematic in nature, i.e., they can affect the signal distributions. The free gauge coupling g_R , on the

other hand, is non-kinematic and only scales the distributions (this is true as long as the narrow-width approximation is valid. Large width can affect various distributions and can potentially change the reach. However, we ignore the large width effects for simplicity). In Fig. 6, the contours correspond to fixed g_R values to achieve 5σ discovery significance, i.e., a region with a particular colour will have signal significance 5σ or more for the corresponding value of g_R . There are two special regions in the plot where the sensitivity is low – one with $M_{N_R} \lesssim M_{W'}$ where the $\text{BR}(W' \rightarrow N_R \ell)$ is phase-space suppressed. It can be checked from Fig. 2. The other region is where $M_{N_R} \lesssim 0.1 \times M_{W'}$. This is the merged region for which a different analysis strategy is required [19].

VI. SUMMARY AND CONCLUSIONS

In this paper, we have studied a hitherto experimentally unexplored signature of the left-right symmetric models with the inverse seesaw mechanism for neutrino mass generation. In particular, we have considered a channel where sequential decays of two TeV-scale new particles, a heavy charged gauge boson, W' and a pseudo-Dirac right-handed neutrino, N_R , lead to a final state with two high- p_T same-flavour-opposite-sign leptons and a W -like fatjet.

A similar process involving a W' and a Majorana N_R , known as the Keung-Senjanović process, has been already searched for at the LHC as a test of lepton number violation. The final state of the KS process is a same-sign lepton pair and a pair of jets. It originates from Drell-Yan production of a W' . The W' first decays to a $N_R \ell$ pair, and then the N_R undergoes through a three-body decay, $N_R \rightarrow \ell jj$ via an off-shell W' . If the RHN is completely Majorana type, both the same-sign and opposite-sign dilepton final states will be present with equal strength, but if it is pseudo-Dirac type, the same-sign dilepton final state will be (almost) absent. There is

a possibility of two-body decays of $N_R \rightarrow \ell W \rightarrow \ell jj$ that gives the same ℓjj final state but through an on-shell W . However, in the standard type-I seesaw mechanism with TeV-scale RHNs, the partial widths of the two-body decay modes of N_R are negligible due to the small Yukawa couplings involved in the decays. In the LRSM, a three-body decay of N_R through off-shell W' opens up, which, despite the phase space suppression, can overcome the two-body decays to become the dominant decay mode of N_R . This leads to the KS process but at the expense of small Yukawa couplings required in the type-I seesaw mechanism to have a TeV-scale N_R in the spectrum.

We invoke the inverse seesaw mechanism to have a natural TeV-scale N_R with order one Yukawa couplings controlling the two-body decays. Consequently, the two-body decay BRs overcome the three-body one when the N_R is embedded in the LRSM. In this setup, we lose the clean same-sign signature of the KS process, but a similar opposite-sign dilepton signature arises whose kinematic nature is very different from the KS process. In association with the lepton pair, we also have a pair of jets similar to the KS process in the final state. However, two jets are collimated in our process as they come from the decay of a boosted W boson. Therefore, our final state contains two same-flavour-opposite-sign leptons and a W -like fatjet. We design a set of selection cuts using the jet-substructure variables to observe the signal over the large background with a significance of more than 5σ at the HL-LHC. We have found that a W' with $g_R \approx g_L$ and mass up to ~ 6 TeV can be discovered at the HL-LHC through this channel.

ACKNOWLEDGMENTS

A.M. acknowledges financial support from SERB-DST, Govt. of India through the project EMR/2017/001434. M.T.A. acknowledges financial support of DST through INSPIRE Faculty grant.

-
- [1] R. N. Mohapatra, *Mechanism for Understanding Small Neutrino Mass in Superstring Theories*, *Phys. Rev. Lett.* **56** (1986) 561–563.
 - [2] R. N. Mohapatra and J. W. F. Valle, *Neutrino Mass and Baryon Number Nonconservation in Superstring Models*, *Phys. Rev. D* **34** (1986) 1642.
 - [3] F. Bazzocchi, *Minimal Dynamical Inverse See Saw*, *Phys. Rev. D* **83** (2011) 093009, [1011.6299].
 - [4] A. G. Dias, C. A. de S. Pires and P. S. R. da Silva, *How the Inverse See-Saw Mechanism Can Reveal Itself Natural, Canonical and Independent of the Right-Handed Neutrino Mass*, *Phys. Rev. D* **84** (2011) 053011, [1107.0739].
 - [5] W.-Y. Keung and G. Senjanovic, *Majorana Neutrinos and the Production of the Right-handed Charged Gauge Boson*, *Phys. Rev. Lett.* **50** (1983) 1427.
 - [6] A. Ferrari, J. Collot, M.-L. Andrieux, B. Belhorma, P. de Saintignon, J.-Y. Hostachy et al., *Sensitivity study for new gauge bosons and right-handed Majorana neutrinos in pp collisions at $\sqrt{s} = 14$ TeV*, *Phys. Rev. D* **62** (2000) 013001.
 - [7] S. N. Gninenko, M. M. Kirsanov, N. V. Krasnikov and V. A. Matveev, *Detection of heavy Majorana neutrinos and right-handed bosons*, *Phys. Atom. Nucl.* **70** (2007) 441–449.
 - [8] A. Atre, T. Han, S. Pascoli and B. Zhang, *The Search for Heavy Majorana Neutrinos*, *JHEP* **05** (2009) 030, [0901.3589].
 - [9] M. Nemevsek, F. Nesti, G. Senjanovic and Y. Zhang, *First Limits on Left-Right Symmetry Scale from LHC Data*, *Phys. Rev. D* **83** (2011) 115014, [1103.1627].
 - [10] C.-Y. Chen and P. S. B. Dev, *Multi-Lepton Collider Signatures of Heavy Dirac and Majorana Neutrinos*, *Phys.*

- Rev. D* **85** (2012) 093018, [1112.6419].
- [11] J. Chakraborty, J. Gluza, R. Seivillano and R. Szafron, *Left-Right Symmetry at LHC and Precise 1-Loop Low Energy Data*, *JHEP* **07** (2012) 038, [1204.0736].
- [12] J. A. Aguilar-Saavedra and F. R. Joaquim, *Measuring heavy neutrino couplings at the LHC*, *Phys. Rev. D* **86** (2012) 073005, [1207.4193].
- [13] T. Han, I. Lewis, R. Ruiz and Z.-g. Si, *Lepton Number Violation and W' Chiral Couplings at the LHC*, *Phys. Rev. D* **87** (2013) 035011, [1211.6447]. [Erratum: *Phys.Rev.D* **87**, 039906 (2013)].
- [14] C.-Y. Chen, P. S. B. Dev and R. N. Mohapatra, *Probing Heavy-Light Neutrino Mixing in Left-Right Seesaw Models at the LHC*, *Phys. Rev. D* **88** (2013) 033014, [1306.2342].
- [15] T. G. Rizzo, *Exploring new gauge bosons at a 100 TeV collider*, *Phys. Rev. D* **89** (2014) 095022, [1403.5465].
- [16] J. Gluza and T. Jeliński, *Heavy neutrinos and the pplljj CMS data*, *Phys. Lett. B* **748** (2015) 125–131, [1504.05568].
- [17] J. N. Ng, A. de la Puente and B. W.-P. Pan, *Search for Heavy Right-Handed Neutrinos at the LHC and Beyond in the Same-Sign Same-Flavor Leptons Final State*, *JHEP* **12** (2015) 172, [1505.01934].
- [18] P. S. B. Dev, D. Kim and R. N. Mohapatra, *Disambiguating Seesaw Models using Invariant Mass Variables at Hadron Colliders*, *JHEP* **01** (2016) 118, [1510.04328].
- [19] M. Mitra, R. Ruiz, D. J. Scott and M. Spannowsky, *Neutrino Jets from High-Mass W_R Gauge Bosons in TeV-Scale Left-Right Symmetric Models*, *Phys. Rev. D* **94** (2016) 095016, [1607.03504].
- [20] A. Roitgrund and G. Eilam, *Search for like-sign dileptons plus two jets signal in the framework of the manifest left-right symmetric model*, *JHEP* **01** (2021) 031, [1704.07772].
- [21] A. Das, P. S. B. Dev and R. N. Mohapatra, *Same Sign versus Opposite Sign Dileptons as a Probe of Low Scale Seesaw Mechanisms*, *Phys. Rev. D* **97** (2018) 015018, [1709.06553].
- [22] C. Arbelaéz, C. Dib, I. Schmidt and J. C. Vasquez, *Probing the Dirac or Majorana nature of the Heavy Neutrinos in pure leptonic decays at the LHC*, *Phys. Rev. D* **97** (2018) 055011, [1712.08704].
- [23] M. Nemevšek, F. Nesti and G. Popara, *Keung-Senjanović process at the LHC: From lepton number violation to displaced vertices to invisible decays*, *Phys. Rev. D* **97** (2018) 115018, [1801.05813].
- [24] V. Brdar and A. Y. Smirnov, *Low Scale Left-Right Symmetry and Naturally Small Neutrino Mass*, *JHEP* **02** (2019) 045, [1809.09115].
- [25] M. J. Dolan, T. P. Dutka and R. R. Volkas, *Dirac-Phase Thermal Leptogenesis in the extended Type-I Seesaw Model*, *JCAP* **06** (2018) 012, [1802.08373].
- [26] J. A. Casas and A. Ibarra, *Oscillating neutrinos and $\mu \rightarrow e, \gamma$* , *Nucl. Phys. B* **618** (2001) 171–204, [hep-ph/0103065].
- [27] A. Mukherjee and N. Narendra, *Realizing flavored leptogenesis: a reappraisal through special kinds of orthogonal matrices*, *2105.14593*.
- [28] P. Konar, A. Mukherjee, A. K. Saha and S. Show, *Linking pseudo-Dirac dark matter to radiative neutrino masses in a singlet-doublet scenario*, *Phys. Rev. D* **102** (2020) 015024, [2001.11325].
- [29] P. Konar, A. Mukherjee, A. K. Saha and S. Show, *A dark clue to seesaw and leptogenesis in a pseudo-Dirac singlet doublet scenario with (non)standard cosmology*, *JHEP* **03** (2021) 044, [2007.15608].
- [30] P. F. de Salas, D. V. Forero, S. Gariazzo, P. Martínez-Miravé, O. Mena, C. A. Ternes et al., *2020 global reassessment of the neutrino oscillation picture*, *JHEP* **02** (2021) 071, [2006.11237].
- [31] A. Mukherjee and M. K. Das, *Neutrino phenomenology and scalar Dark Matter with A_4 flavor symmetry in Inverse and type II seesaw*, *Nucl. Phys. B* **913** (2016) 643–663, [1512.02384].
- [32] A. Mukherjee, D. Borah and M. K. Das, *Common Origin of Non-zero θ_{13} and Dark Matter in an S_4 Flavour Symmetric Model with Inverse Seesaw*, *Phys. Rev. D* **96** (2017) 015014, [1703.06750].
- [33] S. Blanchet, P. S. B. Dev and R. N. Mohapatra, *Leptogenesis with TeV Scale Inverse Seesaw in $SO(10)$* , *Phys. Rev. D* **82** (2010) 115025, [1010.1471].
- [34] A. Das, N. Okada and D. Raut, *Enhanced pair production of heavy Majorana neutrinos at the LHC*, *Phys. Rev. D* **97** (2018) 115023, [1710.03377].
- [35] A. Das, N. Okada and D. Raut, *Heavy Majorana neutrino pair productions at the LHC in minimal $U(1)$ extended Standard Model*, *Eur. Phys. J. C* **78** (2018) 696, [1711.09896].
- [36] D. Choudhury, K. Deka, T. Mandal and S. Sadhukhan, *Neutrino and Z' phenomenology in an anomaly-free $U(1)$ extension: role of higher-dimensional operators*, *JHEP* **06** (2020) 111, [2002.02349].
- [37] K. Deka, T. Mandal, A. Mukherjee and S. Sadhukhan, *Leptogenesis in an anomaly-free $U(1)$ extension with higher-dimensional operators*, *2105.15088*.
- [38] S. Banerjee, P. S. B. Dev, A. Ibarra, T. Mandal and M. Mitra, *Prospects of Heavy Neutrino Searches at Future Lepton Colliders*, *Phys. Rev. D* **92** (2015) 075002, [1503.05491].
- [39] ATLAS collaboration, M. Aaboud et al., *Search for heavy Majorana or Dirac neutrinos and right-handed W gauge bosons in final states with two charged leptons and two jets at $\sqrt{s} = 13$ TeV with the ATLAS detector*, *JHEP* **01** (2019) 016, [1809.11105].
- [40] CMS collaboration, *Search for a right-handed W boson and heavy neutrino in proton-proton collisions at $\sqrt{s} = 13$ TeV*, CMS-PAS-EXO-20-002.
- [41] ATLAS collaboration, M. Aaboud et al., *Search for a right-handed gauge boson decaying into a high-momentum heavy neutrino and a charged lepton in pp collisions with the ATLAS detector at $\sqrt{s} = 13$ TeV*, *Phys. Lett. B* **798** (2019) 134942, [1904.12679].
- [42] CMS collaboration, A. M. Sirunyan et al., *Search for heavy neutrinos and third-generation leptoquarks in hadronic states of two τ leptons and two jets in proton-proton collisions at $\sqrt{s} = 13$ TeV*, *JHEP* **03** (2019) 170, [1811.00806].
- [43] CMS collaboration, A. M. Sirunyan et al., *Search for heavy Majorana neutrinos in same-sign dilepton channels in proton-proton collisions at $\sqrt{s} = 13$ TeV*, *JHEP* **01** (2019) 122, [1806.10905].
- [44] ATLAS collaboration, G. Aad et al., *Search for heavy*

- neutral leptons in decays of W bosons produced in 13 TeV pp collisions using prompt and displaced signatures with the ATLAS detector, *JHEP* **10** (2019) 265, [1905.09787].
- [45] CMS collaboration, Search for long-lived heavy neutral leptons with displaced vertices in pp collisions at $\sqrt{s} = 13$ TeV with the CMS detector, CMS-PAS-EXO-20-009.
- [46] ATLAS collaboration, G. Aad et al., Search for new resonances in mass distributions of jet pairs using 139 fb^{-1} of pp collisions at $\sqrt{s} = 13$ TeV with the ATLAS detector, *JHEP* **03** (2020) 145, [1910.08447].
- [47] CMS collaboration, A. M. Sirunyan et al., Search for high mass dijet resonances with a new background prediction method in proton-proton collisions at $\sqrt{s} = 13$ TeV, *JHEP* **05** (2020) 033, [1911.03947].
- [48] ATLAS collaboration, M. Aaboud et al., Search for $W' \rightarrow tb$ decays in the hadronic final state using pp collisions at $\sqrt{s} = 13$ TeV with the ATLAS detector, *Phys. Lett. B* **781** (2018) 327–348, [1801.07893].
- [49] ATLAS collaboration, M. Aaboud et al., Search for vector-boson resonances decaying to a top quark and bottom quark in the lepton plus jets final state in pp collisions at $\sqrt{s} = 13$ TeV with the ATLAS detector, *Phys. Lett. B* **788** (2019) 347–370, [1807.10473].
- [50] CMS collaboration, A. M. Sirunyan et al., Search for W' bosons decaying to a top and a bottom quark at $\sqrt{s} = 13$ TeV in the hadronic final state, 2104.04831.
- [51] ATLAS collaboration, G. Aad et al., Search for a heavy charged boson in events with a charged lepton and missing transverse momentum from pp collisions at $\sqrt{s} = 13$ TeV with the ATLAS detector, *Phys. Rev. D* **100** (2019) 052013, [1906.05609].
- [52] CMS collaboration, Search for new physics in the lepton plus missing transverse momentum final state in proton-proton collisions at 13 TeV center-of-mass energy, CMS-PAS-EXO-19-017.
- [53] ATLAS collaboration, M. Aaboud et al., Search for High-Mass Resonances Decaying to $\tau\nu$ in pp Collisions at $\sqrt{s} = 13$ TeV with the ATLAS Detector, *Phys. Rev. Lett.* **120** (2018) 161802, [1801.06992].
- [54] CMS collaboration, A. M. Sirunyan et al., Search for a W' boson decaying to a τ lepton and a neutrino in proton-proton collisions at $\sqrt{s} = 13$ TeV, *Phys. Lett. B* **792** (2019) 107–131, [1807.11421].
- [55] ATLAS collaboration, G. Aad et al., Search for heavy resonances decaying into a W boson and a Higgs boson in final states with leptons and b -jets in 139 fb^{-1} of pp collisions at $\sqrt{s} = 13$ TeV with the ATLAS detector, ATLAS-CONF-2021-026.
- [56] ATLAS collaboration, G. Aad et al., Search for resonances decaying into a weak vector boson and a Higgs boson in the fully hadronic final state produced in proton–proton collisions at $\sqrt{s} = 13$ TeV with the ATLAS detector, *Phys. Rev. D* **102** (2020) 112008, [2007.05293].
- [57] CMS collaboration, Search for heavy resonances decaying to WW , WZ , or WH boson pairs in the lepton plus merged jet final state at $\sqrt{s} = 13$ TeV, CMS-PAS-B2G-19-002.
- [58] CMS collaboration, A. M. Sirunyan et al., A multi-dimensional search for new heavy resonances decaying to boosted WW , WZ , or ZZ boson pairs in the dijet final state at 13 TeV, *Eur. Phys. J. C* **80** (2020) 237, [1906.05977].
- [59] ATLAS collaboration, G. Aad et al., Search for diboson resonances in hadronic final states in 139 fb^{-1} of pp collisions at $\sqrt{s} = 13$ TeV with the ATLAS detector, *JHEP* **09** (2019) 091, [1906.08589]. [Erratum: *JHEP* **06**, 042 (2020)].
- [60] ATLAS collaboration, G. Aad et al., Search for heavy diboson resonances in semileptonic final states in pp collisions at $\sqrt{s} = 13$ TeV with the ATLAS detector, *Eur. Phys. J. C* **80** (2020) 1165, [2004.14636].
- [61] T. Mandal, S. Mitra and S. Seth, Single Productions of Colored Particles at the LHC: An Example with Scalar Leptoquarks, *JHEP* **07** (2015) 028, [1503.04689].
- [62] T. Mandal, S. Mitra and S. Seth, Probing Compositeness with the CMS $eejj$ & eej Data, *Phys. Lett. B* **758** (2016) 219–225, [1602.01273].
- [63] T. Mandal, S. Mitra and S. Raz, $R_{D^{(*)}}$ motivated \mathcal{S}_1 leptoquark scenarios: Impact of interference on the exclusion limits from LHC data, *Phys. Rev. D* **99** (2019) 055028, [1811.03561].
- [64] A. Bhaskar, D. Das, T. Mandal, S. Mitra and C. Neeraj, Precise limits on the charge-2/3 $U1$ vector leptoquark, *Phys. Rev. D* **104** (2021) 035016, [2101.12069].
- [65] A. Alloul, N. D. Christensen, C. Degrande, C. Duhr and B. Fuks, FeynRules 2.0 - A complete toolbox for tree-level phenomenology, *Comput. Phys. Commun.* **185** (2014) 2250–2300, [1310.1921].
- [66] C. Degrande, C. Duhr, B. Fuks, D. Grellscheid, O. Mattelaer and T. Reiter, UFO - The Universal FeynRules Output, *Comput. Phys. Commun.* **183** (2012) 1201–1214, [1108.2040].
- [67] J. Alwall, R. Frederix, S. Frixione, V. Hirschi, F. Maltoni, O. Mattelaer et al., The automated computation of tree-level and next-to-leading order differential cross sections, and their matching to parton shower simulations, *JHEP* **07** (2014) 079, [1405.0301].
- [68] T. Sjöstrand, S. Ask, J. R. Christiansen, R. Corke, N. Desai, P. Ilten et al., An introduction to PYTHIA 8.2, *Comput. Phys. Commun.* **191** (2015) 159–177, [1410.3012].
- [69] DELPHES 3 collaboration, J. de Favereau, C. Delaere, P. Demin, A. Giammanco, V. Lemaître, A. Mertens et al., DELPHES 3, A modular framework for fast simulation of a generic collider experiment, *JHEP* **02** (2014) 057, [1307.6346].
- [70] M. Cacciari, G. P. Salam and G. Soyez, The anti- k_t jet clustering algorithm, *JHEP* **04** (2008) 063, [0802.1189].
- [71] M. Cacciari, G. P. Salam and G. Soyez, FastJet User Manual, *Eur. Phys. J. C* **72** (2012) 1896, [1111.6097].
- [72] A. Bhaskar, T. Mandal, S. Mitra and M. Sharma, Improving third-generation leptoquark searches with combined signals and boosted top, 2106.07605.
- [73] S. Catani, L. Cieri, G. Ferrera, D. de Florian and M. Grazzini, Vector boson production at hadron colliders: a fully exclusive QCD calculation at NNLO, *Phys. Rev. Lett.* **103** (2009) 082001, [0903.2120].
- [74] G. Balossini, G. Montagna, C. M. Carloni Calame, M. Moretti, O. Nicrosini, F. Piccinini et al., Combination of electroweak and QCD corrections to single W production at the Fermilab Tevatron and the CERN LHC, *JHEP* **01** (2010) 013, [0907.0276].
- [75] C. Muselli, M. Bonvini, S. Forte, S. Marzani and

- G. Ridolfi, *Top Quark Pair Production beyond NNLO*, *JHEP* **08** (2015) 076, [[1505.02006](#)].
- [76] N. Kidonakis, *Theoretical results for electroweak-boson and single-top production*, *PoS DIS2015* (2015) 170, [[1506.04072](#)].
- [77] J. M. Campbell, R. K. Ellis and C. Williams, *Vector boson pair production at the LHC*, *JHEP* **07** (2011) 018, [[1105.0020](#)].
- [78] A. Kulesza, L. Motyka, D. Schwartzländer, T. Stebel and V. Theeuwes, *Associated production of a top quark pair with a heavy electroweak gauge boson at NLO+NNLL accuracy*, *Eur. Phys. J. C* **79** (2019) 249, [[1812.08622](#)].